

# Design of a ZCT Inverter for a Brushless DC Motor

## Theoretical Analysis

B. Taleb  
School of Engineering & Logistics  
Charles Darwin University  
Darwin Australia 0909  
s994786@students.cdu.edu.au

K. Debnath  
School of Engineering & Logistics  
Charles Darwin University  
Darwin Australia 0909  
kamal.debnath@cdu.edu.au

D. Patterson  
University of Nebraska  
Lincoln  
Nebraska USA  
patterson@ieee.org

### ABSTRACT

*In this paper, a full theoretical and mathematical analysis of a zero current transition inverter (ZCT) for the control of an Axial Flux Brushless DC motor is conducted. The ZCT inverter is applied to control an axial flux brushless DC Motor using a six-step control. In the six-step switching control, one switch in one leg is pulse width modulating while the other in the other leg is kept on for the whole period of commutation. This is done in order to minimize the switching losses in the inverter. A thorough simulation of the inverter is conducted by using MATLAB SIMULINK package. From this, the resonant capacitors, inductors, and the auxiliary MOSFETs switches were selected. After an evaluation of various soft switching techniques, the Zero Current Transition soft Switched PWM inverter was chosen for the work reported in this paper due to its good features. Compared with hard-switching condition, the turn on and turn off loss is reduced. The voltage overshoot and high frequency ringing at the turn off transition is basically eliminated. The resonant capacitor stress is manageable. The current and thermal stresses are distributed evenly among the auxiliary devices. The switching frequency and the current capabilities of the devices are increased. This zero current transition inverter, enables all the main switches, diodes and auxiliary switches to be turned off under zero current transition, and in the main time provides an opportunity to achieve zero voltage turn on for the main switches. While minimising switching losses, which is a major expectation, controlling each phase separately requires no modification to normal PWM algorithms.*

### 1. INTRODUCTION

Brushless DC motors (BLDC) need to be fed from some direct current to alternative current (DC-AC) converters. They are synchronous motors with permanent magnets on the rotor and armature windings on the stator. From a construction point of view, a BLDC is an inside-out version of a DC motor. The latter have permanent magnets or field windings on the stator and the armature windings on the rotor. The most obvious advantage of the (BLDC) is the absence of brushes, which eliminates brush maintenance and also the associated arcing, radio frequency interference (RFI), and electromagnetic interference (EMI). Having the armature windings on the stator helps its cooling. The field excitation is contributed by permanent magnets and does not have to

be supplied by the armature current. Electrical losses in the rotor are therefore eliminated. The efficiency of BLDC motors is significantly better than induction motors in the fractional horsepower range. The former will have better efficiency and better power factor and, therefore a greater output power for the same frame size. These advantages come at the expense of increased complexity in the electronic controller and the need for shaft position sensing. Permanent magnets are thought to be more viable in smaller motors, usually below 20kW. In larger motors, the cost and weight of the magnets could become excessive, and it historically made more sense to opt for excitation by electromagnetic or induction means. However with the development of high-field PM materials, and the rapidly decreasing costs of such materials, PM motors with ratings of a few megawatts have been built. For an axial flux BLDC motor, as the name suggests, the magnetic field that interplays between the stator and the rotor crosses the air gap in the axial direction. The axial geometry of the motor has substantial advantages over the more common radial flux machine for two reasons [10-14, 18]. First, the aspect ratio fits more comfortably into a wheel, and there are significant volume savings over the more usual radial flux geometry, for which much of the internal volume does not contribute to power output. Second and more importantly, a very simple technique for flux weakening that relies on mechanical adjustment of the air gap, and which does not impinge significantly on the efficiency, becomes possible. Within a reasonable band, increasing the air gap increases the copper loss as the torque constant decreases, but decreases the iron loss as the flux density reduces. The motor can be readily dismantled and reassembled with a range of spacers on the shaft, providing different air gaps. BLDC motors are predominantly surface-magnet machines with wide magnet pole arcs and concentrated or distributed stator windings. The design is based on the trapezoidal waveform distribution of the air-gap flux density waveform. A three phase stator winding is constructed in a similar fashion to that of an ac induction motor, it is wound to give a trapezoidal air gap flux in the case of a brushless dc motor and a sinusoidal distribution in the case of a sine-wave wound permanent magnet synchronous motor. The rotor consists of a number of high performance permanent magnets rigidly fixed to the rotor's core structure. The arrangement shapes, and location of the magnets can be modified to give a wide range of motor characteristics. Direct current to alternative current (DC-AC) converters can be classified as hard-switching and soft-switching converters

according to their switching characteristics. In hard-switching AC-DC pulse width modulated (PWM) converters, sudden changes in switch voltage and current waveforms cause severe switching losses and EMI problems. High voltage and current peaks can also be observed during switching transients, because of parasitic capacitance and stray inductance around power devices [1-6]. Medium-power inverters have undergone significant changes. One improvement stems from new power transistors such as insulated-gate-bipolar transistors (IGBTs) with their increasing voltage, current capabilities and switching frequencies. Reactive components i.e. (inductors and capacitors) may be added for filtering out unwanted harmonics and for intermediate energy storage. For these reactive components to be small, for transients to be held at bay and for strict harmonic specifications to be met, the switching frequency of the inverter must be high. A minimum switching frequency of about 16 kHz is necessary in order to keep the filtering within reasonable limit, and the acoustic noise from the motor above the audible range.

## 2. SOFT SWITCHED DC-AC CONVERTERS

Soft-switching techniques have recently been applied in the design of DC-AC converters, in order to achieve better performance, higher efficiency, and higher power density. A substantial number of new topologies for different applications have been developed [7-16]. The topologies classifications are based on the location of the resonant network (load, inverter bridge, and bus), the characteristic of switching waveforms, (zero-voltage switching or zero-current switching), and the type of resonance (series or parallel). Power switches are an integral part of any power converter circuit, unfortunately they are the major source of power dissipation in the circuit. This power dissipation is caused by two features. One is conduction voltage drop in the switch while the switch is conducting the other is due to switching. Some devices, such as metal-oxide-semi-conductor-controlled thyristor (MCT) and bipolar junction transistor (BJT), have lower conduction drop, hence lower conduction losses. Other devices, such as the insulated gate bipolar transistor (IGBT), and the metal-oxide-semi-conductor field effect transistor (MOSFET), have medium to high conduction drops, and hence medium to high conduction losses. Switch-mode power conversion requires high frequency PWM operation to achieve small size, low weight, and excellent dynamic performance of converters. Hard switching results in significant switching losses per cycle, electromagnetic interference (EMI) noise and switching stresses. At high switching frequencies, the total switching losses of power devices and EMI become serious problems. High switching losses reduce power conversion efficiency and result in the need for large heatsinks. The EMI noise may perturb the normal operation of nearby electric/electronic equipment or devices. To alleviate the difficulties associated with hard switching, the concepts of soft switching were introduced. This technology has solved most of the problems associated with high frequency operation of PWM power converters. In a soft-switched converter, in

general, power switches are commutated at voltage zero (zero voltage switching ZVS) or at current zero (zero current switching ZCS) condition or both zero-voltage and zero-current switching (ZVZCS). With these methods, both switching losses and switch stresses can be reduced. However, the operation of the soft switched-converters requires additional active and/or passive elements. This introduces additional cost and complexity. It is a very important and practical issue to determine appropriate soft-switching techniques to meet specific application requirements. The Zero Current Transition soft switched (ZCT) PWM inverter was chosen for the work reported in this paper due to its good features [17]. The voltage and current ratings of the active switches and all the diodes are lower. Each phase leg of the main circuit has a corresponding auxiliary circuit to assist the ZCT operation. Therefore, each switch is commutated independently so that any PWM scheme for hard switching counterparts can be directly employed without modification. Since all the active switches are turned on and off at zero current, power switches with long tailed turnoff currents, such as power transistors and IGBT'S are good candidates for the ZCT topology.

## 3. POWER ELECTRONIC CONVERTER

BLDC motors require a variable-frequency, variable amplitude source that is usually provided by a three-phase, full bridge inverter as shown in Figure 1. The switches could be BJTs, MOSFETS, IGBTs or MCTs. The decreasing cost and dramatic improvement in performance of these semiconductor devices have accelerated the application of BLDC motor drives. The inverter is usually responsible for both the electronic commutation and current regulation. The position information obtained from the position sensors is used to open and close the six inverter switches for commutation. As the motor windings are star connected and the star point is isolated, the inverter input current flows through two of the three phases in series at any time. Hysteresis or pulse-width-modulated current controllers are typically used to regulate the actual machine currents to the rectangular current reference waveforms. When  $S_1$  and  $S_6$  are on their on state, the current builds up in the path  $S_1$ , phase A, phase B, and  $S_6$ . When switch  $S_1$  is turned off, the current then decays through the body diode  $D_4$  of  $S_4$  and switch  $S_6$ . Alternatively  $S_6$  could be turned off, and the current would then decay in the loop formed by  $S_1$  and body diode  $D_3$  of  $S_3$ . The stator excitation for BLDC motors needs to be synchronized with rotor speed and position to produce constant torque. The controller has to keep track of the rotor angular position and switch the excitation among the motor phases appropriately. It performs the role of the mechanical commutator of a DC machine. For this reason brushless DC motors are also called electronically commutated motors. The rotor position needs to be detected at six discrete points in each electrical cycle, i.e.  $60^\circ$  electrical intervals for the commutation. The most common method of sensing the rotor position is by using Hall effect sensors. A Hall effect sensor consists of a set of Hall switches and a set of trigger magnets. The Hall effect switch is a

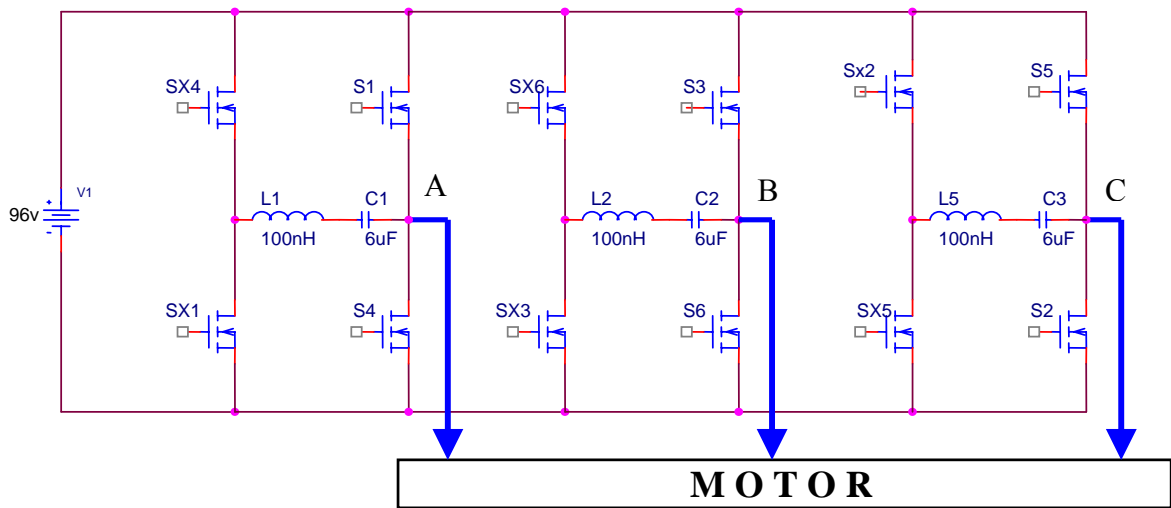


**Figure 1** Schematic diagram of a three-phase ZCT inverter

semiconductor device based on the Hall effect that opens or closes when the magnetic field is higher or lower than a threshold value. A signal conditioning circuit integrated with the Hall effect switch provides a TTL compatible pulse with sharp edges and high noise immunity for connection to the controller. For a three-phase BLDC motor, three Hall effect switches spaced  $120^\circ$  electrical degree apart are mounted on the stator. The trigger magnets can be a separate set of magnets aligned with the rotor magnets and mounted on the shaft in close proximity to the Hall effect switches. The rotor magnets can also be used as trigger magnets. The Hall effect switches are mounted close enough to be energized by the leakage flux at the appropriate rotor positions. The digital signals from the Hall effect sensors are then decoded to obtain the three-phase switching sequence for the inverter. High-resolution encoders or revolvers can also be used to provide position feedback. Their cost being high, they are only justified where sinusoidal drive is required. The ability to operate with just three Hall sensors gives the trapezoidal brushless permanent magnet motor an edge over its sinusoidal counterpart (PMSM) in low cost applications. It should be mentioned that PMSM motors are sometimes operated with rectangular currents to minimize the cost of the position sensor although the output torque waveform is far from the ideal because of the mismatch between the motor and the inverter.

#### 4. MATHEMATICAL ANALYSIS OF THE ZCT INVERTER

As stated earlier, each phase leg of the main circuit has a corresponding auxiliary circuit to assist the ZCT operation. Therefore each phase leg of the main circuit can be controlled independently without modifying the normal PWM scheme. This scheme makes full use of the two auxiliary switches. The switch  $S_{x1}$  is triggered for turning on  $S_1$  and  $S_{x2}$  is triggered for turning it off respectively. The circuit can also solve the diode reverse recovery problem at the main switch turn on transition. The ZCT inverter realizes a balanced stress

distribution in devices and reduces the maximum resonant capacitor voltage. In order to simplify the analysis of the inverter we assume the inductance of the motor is large enough to keep the load current constant during the transition intervals. Also we assume the switches are very fast and their on resistance is negligible so is the tank resistance. We start in the mode of conduction where the body diode  $D_2$  of  $S_2$  conducts the load current. The simulated current  $i_x$  in the resonant tank circuit of the inverter is shown in Figure 2. The eleven topological stages are shown in Figure 3 [17]. Reference 17 talks about hard-switching whereas the inverter scheme reported in this paper describes soft-switching operation.

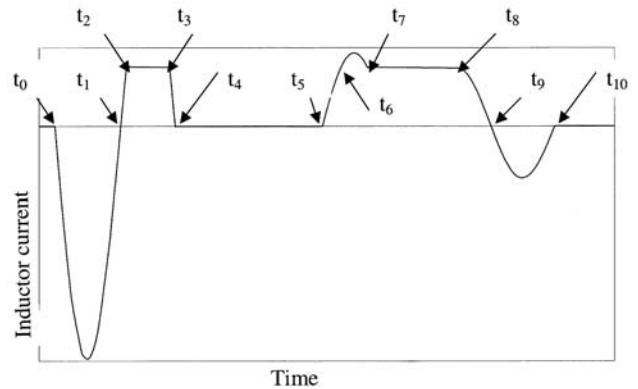


**Figure 2** Simulated current in the resonant tank inductor

##### Interval $t_0$ - $t_1$

The voltage of the resonant circuit across the capacitor  $C_x$  is designated as  $v_x$ . Capacitor  $C_x$  is initially charged to  $V_0 = V_{dc}$  with its left terminal being positive and the initial current  $i_x$  in the tank circuit is nil. To minimize the turn on loss, we apply a gate drive signal to the switch  $S_{x1}$  at  $t = t_0$ . The equivalent circuit is shown in Figure 3(a). A resonant circuit is formed by the circuit,  $S_{x1}$ ,  $L_x$ ,  $C_x$  and the body diode  $D_2$  of switch  $S_2$ .

By applying Kirchoff's Voltage Law (KVL) to the circuit we get:

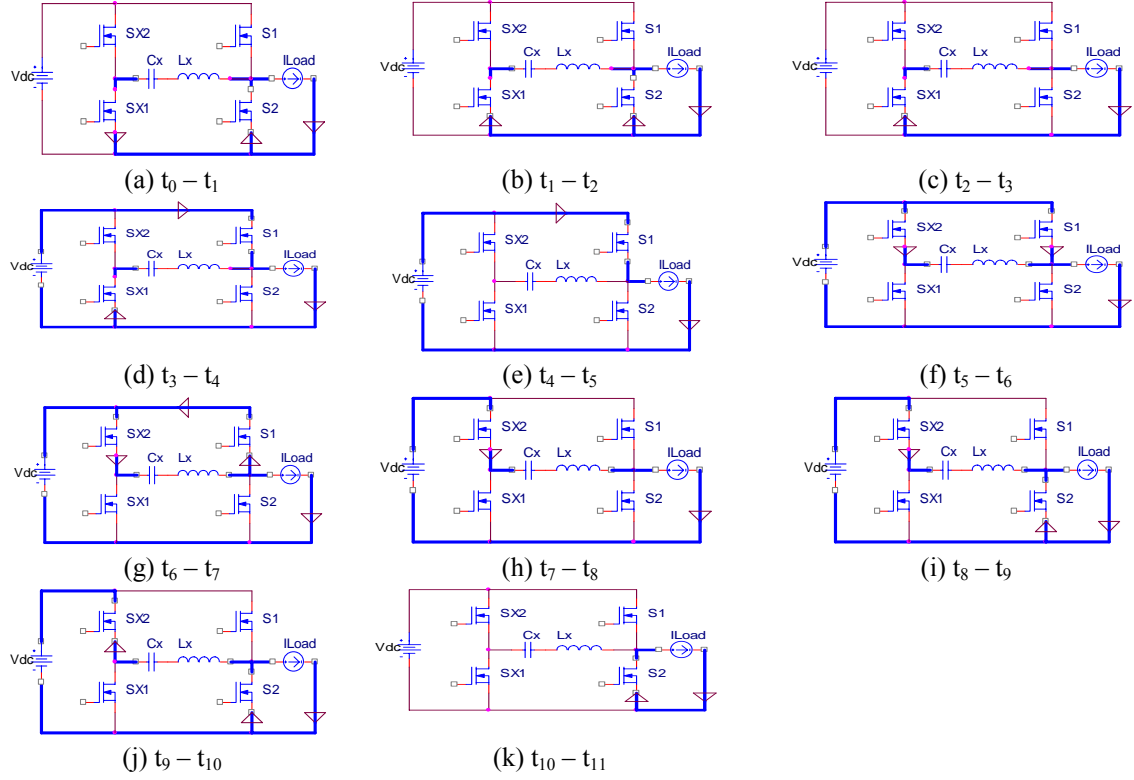


**Figure 3** Topological steps of the commutation of the ZCT Inverter

$$v_x + L_x \frac{di_x}{dt} = 0 \quad (1)$$

The solution of this differential equation is:

$$i_x = -\frac{V_0}{Z} \sin \omega_r t \quad (2)$$

$$v_x = V_0 \cos \omega_r t \quad (3)$$

$$Z = \sqrt{\frac{L_x}{C_x}}, \omega_r L_x = \frac{1}{\omega_r C_x} \quad (4)$$

Where  $Z$  is the characteristic impedance and  $\omega_r$  is the resonance frequency.

$$\omega_r = \frac{1}{\sqrt{L_x C_x}} \quad (5)$$

The current builds up in the negative direction, reaches a maximum and goes back to zero again at the time  $t = t_1$ .

$$i_x(t_1) = -\frac{V_0}{Z} \sin \omega_r (t_1 - t_0) = 0 \quad (6)$$

$$v_x(t_1) = V_0 \cos \omega_r (t_1 - t_0) \quad (7)$$

#### Interval $t_1-t_2$

The equivalent circuit is shown in Figure 3(b). After time  $t = t_1$ , the current builds up in the positive direction and the body diode of the switch  $S_{x1}$  starts to conduct as shown in Figure 3 (b). At time,  $t = t_2$ ,  $i_x$  reaches  $i_{load} = I_d$ , the body diode  $D_2$  of  $S_2$  stops conducting and its current is commutated to the resonant circuit. At time  $t = t_2$  the resonant current  $i_x$  is:

$$i_x(t_2) = I_d = -\frac{V_0}{Z} \sin \omega_r (t_2 - t_0) \quad (8)$$

The capacitor voltage goes negative with its maximum being when  $i_x=0$ . At time  $t = t_2$  the capacitor voltage is still negative:

$$v_x(t_2) = V_0 \cos \omega_r (t_2 - t_0) \quad (9)$$

#### Interval $t_2-t_3$

The equivalent circuit is shown in Figure 3(c). During this interval the diode  $D_2$  has stopped conducting and the capacitor is charging linearly by the constant current in the load. During this interval the current  $i_x$  and the voltage  $V_x$  are respectively equal to:

$$i_x = I_d = i_{load} \quad (10)$$

$$v_x = \frac{1}{C} \int I_d dt = \frac{I_d}{C} t + v_x(t_2) \quad (11)$$

At time  $t = t_3$

$$v_x(t_3) = \frac{I_d}{C} (t_3 - t_2) + v_x(t_2) \quad (12)$$

#### Interval $t_3-t_4$

The equivalent circuit is shown in Figure 3(d). The main switch  $S_1$  is turned on, its current goes up and the current  $i_x$  goes down. At time  $t = t_4$ , the current in the

switch  $S_1$  reaches the load current and the current  $i_x$  falls to zero.

The equation of the circuit is:

$$V_{dc} + v_x + \frac{L di_x}{dt} = 0 \quad (13)$$

$$i_x = \frac{V_{dc} - v_x(t_3)}{Z} \sin \omega_r t + I_d \cos \omega_r(t) \quad (14)$$

$$v_x = V_{dc} + Z \times I_d \sin \omega_r t - (V_{dc} - v_x(t_3)) \cos \omega_r t \quad (15)$$

At  $t = t_4$

$$i_x = 0$$

$$v_x(t_4) = V_{dc} + Z \times I_d \sin \omega_r(t_4 - t_3) - (V_{dc} - v_x(t_3)) \cos \omega_r(t_4 - t_3) \quad (16)$$

The turn on transition is finished.

#### Interval $t_4 - t_5$

The equivalent circuit is shown in Figure 3(e). During this interval, the main switch  $S_1$  is conducting the load current  $I_d$  and the capacitor is charged to  $v_x(t_5) = -V_{dc}$  if the time is sufficient, and the current in the tank  $i_x = 0$

#### Interval $t_5 - t_6$

To soft switch  $S_1$  during its turn off transition  $S_{x2}$  is turned on. The equivalent circuit is shown in Figure 3(f). A resonant circuit is formed through the circuit  $S_1, S_{x2}, L_x$  and  $C_x$ . The equation of the circuit is:

$$v_x + L_x \frac{di_x}{dt} = 0 \quad (17)$$

$$i_x = \frac{-v_x(t_5)}{Z} \sin \omega_r t + I_d \cos \omega_r t \quad (18)$$

$$v_x = Z \times I_d \sin \omega_r t + v_x(t_5) \cos \omega_r t \quad (19)$$

At time  $t = t_6$ ,  $i_x$  reaches  $I_d$  and the switch  $S_1$  stops conducting.

$$i_x(t_6) = \frac{-v_x(t_5)}{Z} \sin \omega_r(t_6 - t_5) + I_d \cos \omega_r(t_6 - t_5) = I_d \quad (20)$$

$$v_x(t_6) = Z \times I_d \sin \omega_r(t_6 - t_5) + v_x(t_5) \cos \omega_r(t_6 - t_5) \quad (21)$$

#### Interval $t_6 - t_7$

The current  $i_x$  continues to grow up to reach its maximum value and falls again to  $I_d$ . The equivalent circuit is shown in Figure 3(g). The body diode of the switch  $S_1$  is conducting. At the end of this interval we have:

$$i_x(t_7) = \frac{-v_x(t_6)}{Z} \sin \omega_r(t_7 - t_6) + I_d \cos \omega_r(t_7 - t_6) \quad (22)$$

$$v_x(t_7) = Z \times I_d \sin \omega_r(t_7 - t_6) + v_x(t_6) \cos \omega_r(t_7 - t_6) \quad (23)$$

#### Interval $t_7 - t_8$

The body diode of switch  $S_1$  has stopped conducting, and the capacitor is charging linearly with the constant current  $I_d$  as shown in Figure 3(h).

At time  $t = t_8$ , we have:

$$v_x(t_8) = \frac{1}{C} \int_{t_7}^{t_8} I_d dt + v_x(t_7) \quad (24)$$

$$i_x = I_d \quad (25)$$

#### Interval $t_8 - t_9$

The diode  $D_2$  starts to conduct. A resonant circuit is formed  $S_{x2}, L_x, C_x, D_2$  and  $V_{dc}$  as shown in Figure 3(i)

$$i_x = \frac{V_{dc} - v_x(t_8)}{Z} \sin \omega_r(t) + I_d \cos \omega_r(t) \quad (26)$$

$$v_x = V_{dc} + Z \times I_d \sin \omega_r(t) - (V_{dc} - v_x(t_8)) \cos \omega_r(t) \quad (27)$$

At  $t = t_9$  we have:

$$i_x(t_9) = \frac{V_{dc} - v_x(t_8)}{Z} \sin \omega_r(t_9 - t_8) + I_d \cos \omega_r(t_9 - t_8) \quad (28)$$

$$v_x(t_9) = V_{dc} + Z \times I_d \sin \omega_r(t_9 - t_8) - (V_{dc} - v_x(t_8)) \cos \omega_r(t_9 - t_8) \quad (29)$$

#### Interval $t_9 - t_{10}$

The current in the auxiliary switch  $S_{x2}$  is going negative and its body diode starts conducting as shown in Figure 3(j). The current and the voltage in the resonant circuit at the end of the interval are:

$$i_x(t_{10}) = \frac{V_{dc} - v_x(t_9)}{Z} \sin \omega_r(t_{10} - t_9) + i_x(t_9) \cos \omega_r(t_{10} - t_9) \quad (30)$$

$$v_x(t_{10}) = V_{dc} + Z i_x(t_9) \sin \omega_r(t_{10} - t_9) - (V_{dc} - v_x(t_9)) \cos \omega_r(t_{10} - t_9) \quad (31)$$

#### Interval $t_{10} - t_{11}$

The body diode of the switch  $S_{x2}$  has stopped conducting, the current in diode  $D_2$  is equal to  $I_d$  as shown in Figure 3(k). The current in the tank  $i_x$  is therefore zero, and the voltage across the capacitor is equal to the initial voltage and the circuit is ready for the next commutation.

The inverter requires four MOSFETs, six 1  $\mu$ F capacitors, one 100 nH inductor and two current transducers in each phase and three electrolytic 4,700  $\mu$ F bus capacitors. The cost of all these items is around 3,000 dollars.

## 5. CONCLUSIONS

The mathematical analysis of a ZCT inverter has been presented. This gives a very good insight to the eleven topological steps of its commutation. All the very good features of the ZCT inverter are listed in Table 1. As can be seen from this table, the improved inverter seems to have the best features which are the zero current transition at turn on and at turn off, a balanced stress on the auxiliary switches, and the smallest resonant voltage across the capacitor. All these features make it a good candidate for its application in the control of a brushless DC motor driving an electrical vehicle in an "in the wheel" design. There will also be some savings in volume. In order to gain an idea of the operating performance of this inverter, computer

simulation was carried out using Simulink software and the results are presented in Reference [18].

**Table 1** Features of the ZCT inverter

Component operation	ZCT feature
Diode turn off	Zero current transition
Main switch turn on	Zero current transition with reduced voltage
Main switch turn off	Zero current transition
Auxiliary switch turn on	Zero current transition
Auxiliary switch turn off	Zero current transition
Auxiliary switch voltage	$V_{dc}$
Auxiliary switch stress	Balanced
Resonant capacitor voltage	$1.3 \times V_{dc}$

## REFERENCES

- [1] Jianwen Shao, Ray L. Lin, Fred C. Lee, Dan Y.Chen, "Characterization of EM Performance for Hard and Soft-switched Inverters" APEC 2000, New Orleans, vol. 2, 6-10 February 2000, pp. 1009-1014.
- [2] D. M. Divan, "The Resonant DC Link Converter-a new Concept in Static Power Conversion," in conference Record of the 1986 IEEE Industry Applications Society Annual Meeting, September/October 1986, pp.648-656
- [3] Axel Mertens, and D. M. Divan, "A High Frequency Resonant DC Link Inverter Using IGBTs," in International Power Electronic conference, Tokyo, 1990, pp.152-160.
- [4] D. M. Divan, and G. Skibinski, "Zero Switching Loss Inverters for High Power Applications," in Conference record of the 1987 IEEE Industry Applications Society annual meeting, 2-7 October 1987, and pp.627-634.
- [5] Alexander Kurnia, Hassan Cherradi, and Deepakraj M. Divan, "Impact of IGBTs Behaviour on Design Optimisation of Soft Switching Inverter Topologies," IEEE On Industry Applications, vol.31, no. 2, March/April 1995, pp. 280-286
- [6] Yimin Jiang, Guichao Hua, Eric Yang, and Fred C. Lee, "Soft-Switching of IGBT's With the Help of MOSFET's in Bridge Type Converters," IEEE 1993 pp. 151-157.
- [7] Guichao Hua, Fred C. Lee, "Soft-Switching Techniques in PWM Converters," IEEE Transactions on Industrial Electronics, vol.42, no. 6, December 1995, pp. 595-603.
- [8] Thomas G. Wilson, "The Evolution of Power Electronics," IEEE Transactions on Power Electronics, vol. 15, no. 3, May 2000, pp. 439-446 Alexander Kurnia, Hassan Cherradi, and Deepakraj M. Divan, "Impact of IGBTs Behaviour on Design Optimisation of Soft Switching Inverter Topologies," IEEE on Industry Applications, vol.31, no. 2, March/April 1995, pp. 280-286.
- [9] Deepakraj M. Divan, Giri Venkataramanan, and Rik W. A. A. De Doncker, "Design Methodologies for Soft Switched Inverters," IEEE Transactions on Industry Applications, vol. 29, no. 1, January/February 1993, pp. 126-134.
- [10] C. Chen, G. A. Luckjiff, G. Vankataramanan, and D. M. Divan, "System Design Issues for Resonant DC Link Inverter Based Drives," at the Conference of the European Power Electronics Association, Brighton, 13-16 September 1993, pp. 182-187.
- [11] Y. Murai, and T.A Lipo, "High Frequency Series Resonant DC Link Power Conversion," in IEEE-IAS 1988, pp. 772-779.
- [12] Renee Spee, and Alan K. Wallace, "Performance Characteristics of Brushless DC Drives," IEEE Transactions on Industry Applications, vol. 24, no. 4 July/August 1988, pp. 568-573.
- [13] Carlos Marcelo de Oliveira Stein, and Helio Leaes Hey, "A True ZCZVT Commutation Cell for PWM Converters," IEEE Transactions on Power Electronics, vol. 15, no. 1, January 2000, pp.185-193.
- [14] M. D. Bellar, Wu. T. S Tchamdjou, A. Mahdavi, and J. M Ehsani, "A Review of Soft Switched DC-AC Converters," IEEE Transactions on Industry Applications, vol. 34, no. 4, July/August 1998, pp. 847-860
- [15] Schonknecht and Rik W. A. A. De Doncker, "Novel Topology for Parallel Connection of Soft-Switching High-Power High-Frequency Inverters," IEEE Transactions on Industry Applications, vol. 34, no. 4, March/April 2003, pp. 550-555.
- [16] Yon Li, Fred C. Lee, Jason Lai, and Dushan Boroyevich, "A Novel Three-Phase Zero-current-Transition and Quasi-Zero-Voltage-Transition ZVT-QZVT) Inverter/Rectifier with Reduced Stresses on Devices and Components," Presented In Fifteenth Annual IEEE Applied Power Electronics Conference and Exposition, New Orleans, Louisiana, 6-10 February, pp. 1031 -1036.
- [17] D. Patterson, X Yan, and S. Camilleri, "A Very High Efficiency Controller For Axial Flux Permanent Magnet Wheel Drive in a Solar Powered Vehicle", IEEE International Conference on Power Electronics Drives and Energy Systems for Industrial Growth, Perth, Australia, 1998, IEEE Conf Proceedings, Vol 2 pp886 - 891
- [18] B. Taleb, K. Debnath and D. Patterson, "Design of a ZCT Inverter for a Brushless DC Motor Simulation Results," to be Presented in AUPEC, Tasmania, Australia, September 2005.